diabetes
American Diabetes Association

Dysregulation of CXCL1 Expression and Neutrophil Recruitment in Insulin Resistance and Diabetes-Related Periodontitis in Male Mice

Takanori Shinjo, Satoru Onizuka, Yumi Zaitsu, Atsushi Ishikado, Kyoungmin Park, Qian Li, Hisashi Yokomizo, Tatsuro Zeze, Kohei Sato, Ronald St-Louis, Jialin Fu, Wu I-Hsien, Koji Mizutani, Hatice Hasturk, Thomas E. Van Dyke, Fusanori Nishimura, and George L. King

Diabetes 2023;72(7):986–998 | https://doi.org/10.2337/db22-1014

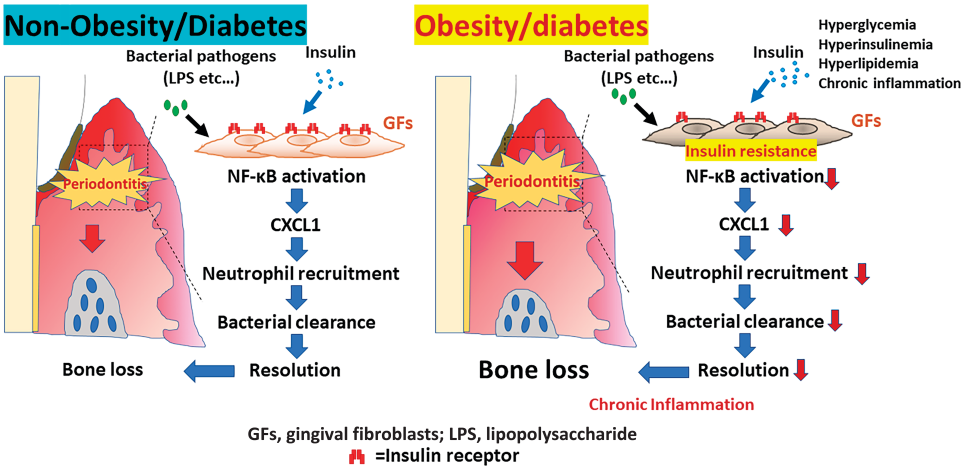

Dysregulation of CXCL1 Expression and Neutrophil Recruitment in Insulin Resistance and Diabetes-Related Periodontitis in Male Mice

Takanori Shinjo,[1,2] Satoru Onizuka,[1] Yumi Zaitsu,[1] Atsushi Ishikado,[1] Kyoungmin Park,[1] Qian Li,[1] Hisashi Yokomizo,[1] Tatsuro Zeze,[2] Kohei Sato,[2] Ronald St-Louis,[1] Jialin Fu,[1] Wu I-Hsien,[1] Koji Mizutani,[3] Hatice Hasturk,[4] Thomas E. Van Dyke,[4] Fusanori Nishimura,[2] and George L. King[1]

Diabetes 2023;72:986–998 | https://doi.org/10.2337/db22-1014

Insulin resistance and hyperglycemia are risk factors for periodontitis and poor wound healing in diabetes, which have been associated with selective loss of insulin activation of the PI3K/Akt pathway in the gingiva. This study showed that insulin resistance in the mouse gingiva due to selective deletion of smooth muscle and fibroblast insulin receptor (SMIRKO mice) or systemic metabolic changes induced by a high-fat diet (HFD) in HFD-fed mice exacerbated periodontitis-induced alveolar bone loss, preceded by delayed neutrophil and monocyte recruitment and impaired bacterial clearance compared with their respective controls. The immunocytokines, CXCL1, CXCL2, MCP-1, TNFα, IL-1β, and IL-17A, exhibited delayed maximal expression in the gingiva of male SMIRKO and HFD-fed mice compared with controls. Targeted overexpression of CXCL1 in the gingiva by adenovirus normalized neutrophil and monocyte recruitment and prevented bone loss in both mouse models of insulin resistance. Mechanistically, insulin enhanced bacterial lipopolysaccharide-induced CXCL1 production in mouse and human gingival fibroblasts (GFs), via Akt pathway and NF-κB activation, which were reduced in GFs from SMIRKO and HFD-fed mice. These results provided the first report that insulin signaling can enhance endotoxin-induced CXCL1 expression to modulate neutrophil recruitment, suggesting CXCL1 as a new therapeutic direction for periodontitis or wound healing in diabetes.

ARTICLE HIGHLIGHTS

- The mechanism for the increased risks for periodontitis in the gingival tissues due to insulin resistance and diabetes is unclear.
- We investigated how insulin action in gingival fibroblasts modulates the progression of periodontitis in resistance and diabetes.
- Insulin upregulated the lipopolysaccharide-induced neutrophil chemoattractant, CXCL1, production in gingival fibroblasts via insulin receptors and Akt activation.
- Enhancing CXCL1 expression in the gingiva normalized diabetes and insulin resistance-induced delays in neutrophils recruitment and periodontitis.
- Targeting dysregulation of CXCL1 in fibroblasts is potentially therapeutic for periodontitis and may also improve wound healing in insulin resistance and diabetes.

Delayed resolution of infections is a major contributor to chronic inflammation and poor wound healing in diabetes and insulin resistance (1,2). A major example of delayed resolution of infections and chronic inflammation is periodontitis, which causes loss of teeth and poor nutrition, even mortality, in older people with diabetes (3–6). Periodontitis is one of the most common noncommunicable diseases and is associated with aging, obesity, nephropathy, and cardiovascular outcomes (7–11). Risk factors for periodontitis in diabetes are hyperglycemia, diabetes duration, and insulin resistance (12). Insulin's beneficial effects to

[1]Section of Vascular Cell Biology, Joslin Diabetes Center, Harvard Medical School, Boston, MA
[2]Section of Periodontology, Faculty of Dental Science, Kyushu University, Fukuoka, Japan
[3]Department of Periodontology, Graduate School of Medical and Dental Sciences, Tokyo Medical and Dental University, Tokyo, Japan
[4]Department of Applied Oral Science, The Forsyth Institute, Cambridge, MA
Corresponding author: George L. King, george.king@joslin.harvard.edu

Received 10 December 2022 and accepted 5 April 2023
This article contains supplementary material online at https://doi.org/10.2337/figshare.22596181.

resolve periodontitis and wound healing are attributed to glycemic control and its direct actions on cell types involved in infection and inflammation (13). However, insulin's direct action to enhance its anti-infectious and anti-inflammatory activities in gingival myofibroblasts and tissues to mitigate periodontitis has not been elucidated.

We reported that, in the gingiva of Zucker fatty rats, a model of obesity-induced diabetes and insulin resistance, insulin signaling to activate eNOS (p-eNOS) was impaired because of selective inhibition of the PI3Kinase/Akt pathway (14). Mice with diet-induced obesity and type 2 diabetes exhibited more severe periodontitis-induced alveolar bone loss and delayed wound healing than controls (15–17). Clinically, people with insulin resistance, without diabetes, have increased risk for severe periodontitis (18). However, it is unclear which type of gingival cells are responding to insulin and how those responses contribute to the development and exacerbation of periodontitis.

This study characterized the direct effect of insulin actions on the development of periodontitis by deletion of insulin receptors (IR) in myofibroblasts of mice (SMIRKO), a major gingival cell type that is activated during injury in periodontitis (19).

RESEARCH DESIGN AND METHODS

Materials

The primary antibodies and reagents (all analytical grade) are listed in Supplementary Tables 1 and 2.

Animals

SM22α-Cre$^{+/-}$IR$^{fl/fl}$ (SMIRKO) mice were generated by breeding IR$^{fl/fl}$ mice with SM22-Cre$^{+/-}$IR$^{fl/fl}$ mice, as reported (20). Male SMIRKO and SM22α-Cre$^{-/-}$IR$^{fl/fl}$ (wild type [WT]) littermates were fed with regular diet (RD). Male WT littermates at 6-weeks-old age were fed with 60% high-fat diet (HFD) (D12492; Research Diet, New Brunswick, NJ) for 10 weeks. All mice were housed under climate-controlled conditions with a 12-h light/dark cycle and with food and water ad libitum. These primers were used for genotyping: floxed IR forward 5′-GATGTGCACCCCATGTCT-3′, reverse 5′-CTGAATAGCTGAGACCACAG-3′, and floxed IR delta 5′-TCTATCAACCGTGCCTAGAG-3′. Mice were perfused with 20 mL PBS. Gingivae around maxilla and mandibular molars were dissected and used for experiments. Intraperitoneal glucose tolerance tests (IPGTTs) and insulin tolerance tests (IPITTs) and ex vivo insulin or IGF-1 stimulation on gingiva were performed as reported (14,20). All protocols for animal use and euthanasia were approved by the Animal Care Committee of the Joslin Diabetes Center (Boston, MA) (#2017-02) and are in accordance with National Institutes of Health (NIH) guidelines.

Immunoblotting and Assays

Gingival samples, snap frozen on dry ice, and cultured cells were homogenized in ice-cold radioimmunoprecipitation assay buffer (Boston BioProducts, Milford, MA) buffer with protease (Sigma-Aldrich) and phosphatase inhibitors, with protein concentrations determined by bicinchoninic acid (BCA) protein assay kit (Thermo Fisher Scientific, Rockford, IL). Immunoblotting was performed and analyzed using ImageJ software (NIH), as described (20). Murine and human CXCL1 (R&D Systems, Minneapolis, MN), and plasma insulin and IGF-1 levels (Crystal Chem, Elk Grove Village, IL) were determined by ELISA kit according to the manufacturer's instruction.

Induction of Periodontitis

At 14 weeks of age, male WT, SMIRKO, and HFD-fed mice were randomly divided into groups with or without 7-0 silk ligature around maxillary second molars to induce experimental periodontitis (Supplementary Fig. 1*A*), as reported (21,22). Each cage contained both WT and SMIRKO mice to stabilize their oral microbiome. After 4, 7, or 14 days, mice were euthanized under anesthesia and perfused with PBS. Assessment of periodontitis by alveolar bone loss (Supplementary Fig. 1*B*) and histological analysis were performed as reported (21,23). RD-fed male C57BL/6, ApoE$^{-/-}$ (Jackson Laboratory, Bar Harbor, ME), and SM22Cre$^{+/-}$-ApoE$^{-/-}$ mice at 14 weeks old were also studied to determine the effect of Cre recombinase on alveolar bone loss.

Histological Analysis

Left hemisected maxillae were fixed in 10% neutral buffered formalin and decalcified in 10% EDTA(23). Paraffin-embedded sections were subjected to tartrate-resistant acid phosphatase (TRAP) stain to detect osteoclastic activity. Methods for obtaining bone marrow–derived macrophages (BMDMs) and differentiation into osteoclasts were as described (24). Active osteoclasts were defined as multinucleated (>2) and TRAP-positive cells in contact with the bone surface (25) or on a plate.

Real-Time PCR

Total RNA was isolated using PureLink RNA Mini kit or TRIzol reagent (Thermo Fisher Scientific) and subjected to real-time PCR to assess mRNA levels (Applied Biosystems, Grand Island, NY) normalized to mouse 18S rRNA. The sequences of PCR primers are listed in Supplementary Table 3.

Flow Cytometry

Gingivae were prepared for FACS analysis as reported (26). Spleen was grounded using a 70-μm strainer; 100 μL blood and bone marrow were suspended in ACK Lysing buffer (Thermo Fisher Scientific) for 5 min at 37°C. Antibodies for FACS and gating strategies are shown in Supplementary Table 1 and Supplementary Fig. 2. Cells were sorted using LSR2 (BD Biosciences, San Jose, CA), and cell populations were determined using Flow Jo software version 10.0 (Tree Star Inc., Ashland, OR).

Primary Gingival Fibroblast Cultures

Mouse gingiva was immersed in PBS containing penicillin and streptomycin, dissected into small pieces, suspended in DMEM containing 10% BSA, and placed on a collagen

I–coated plate. Primary gingival fibroblasts (GFs), passages 3–6, from male WT/SMIRKO/HFD mice were cultured in 0.1% FBS DMEM with low glucose (5.5 mmol/L) (DMEM-L) overnight before treatment with insulin or IGF-1 (0–100 nmol/L) for 10 min for analyses. Cells were stimulated with *Escherichia coli* lipopolysaccharide (LPS), Pam3CSK4, and TNFα (10 ng/mL) at the indicated time (6–24 h for quantitative PCR [qPCR] and 10 h for ELISA) and pretreated with insulin and each inhibitor for 30 min. Cells were stimulated with 0–1,000 ng/mL *E. coli* LPS for 30 min, with or without insulin pretreatment. Human primary GFs were obtained from ATCC (PCS-201-018; Manassas, VA) and cultured according to the manufacturer's protocol.

Immunocytohistology Studies

GFs from male WT/SMIRKO mice were cultured in glass chambers (Nunc Lab-Tek Chamber Slide; Thermo Fisher Scientific) and fixed with 4% paraformaldehyde and treated with PBS containing 0.1% Triton-X100 (Sigma-Aldrich) (PBST) for 10 min. Then, cells were incubated with primary antibodies diluted in 1% BSA in PBST overnight at 4°C, washed, and incubated with secondary antibodies for 1 h, and mounted with a DAPI kit (Agilent, Santa Clara, CA).

Adenoviral Transduction/Intragingival Adenovirus Injection

Adenovirus expressing mouse CXCL1 (no. 188914A) and cytomegalovirus (CMV) null adenovirus (no. 000047A) were purchased (ABM, Richmond, British Columbia, Canada). GFs from male WT mice were infected with adenovirus(1×10^8 inclusion-forming units/mL) for 1 h at 37°C and incubated with 10% FBS DMEM-L with PC/SM for 48 h. Intragingival adenovirus injections were performed as described (27). Briefly, anesthetized mice were injected with a total 20 μL of 1×10^8 inclusion-forming units/mL adenovirus into the palatal gingiva on the right side (Supplementary Fig. 1*C*), and CMV null adenovirus was injected into the left side. For interventional study, ligatured or nonligatured mice were concomitantly injected with adenovirus intragingivally as above. Noninjected mandibular gingiva samples were used as a control.

Lentiviral shRNA Transfection

Lentivirus short hairpin (sh) Akt1 (ABIN3775910) and shCMV (ABIN5691888) were from Antibodies-online GmbH (ABIN3775910; Aachen, Germany). shRNA transfection was performed using the Ambion Silencer Select Validated siRNA kit in 70% confluent GFs, which were selected with puromycin (InvivoGen, San Diego, CA) for 7 days and used for analysis.

Statistical Analysis

Values are expressed as mean ± SEM. Comparisons between two groups were performed with an unpaired Student *t* test. One-way and two-way ANOVA, followed with post hoc tests, were performed for comparisons of multiple groups using GraphPad Prism8 (GraphPad Software, San Diego, CA).

Data and Resource Availability

Data sets and resources generated during this study are available from the corresponding author.

RESULTS

Systemic and Gingival Characterization of SMIRKO Mice

Male SMIRKO and WT mice (Fig. 1*A*) exhibited similar body weights, and blood glucose, fasting plasma insulin, and IGF-1 levels (Supplementary Fig. 3*A–E*). No changes were observed in IPGTT and IPITT (Supplementary Fig. 3*F* and *G*) between these two types of mice, as reported (20). Only male mice were studied in all the experiments.

Gingiva protein levels of IRβ from SMIRKO mice decreased by 73% compared with WT mice ($P < 0.05$), but IGF-1Rβ expression was not different (Fig. 1*B*). Ex vivo study showed that insulin-mediated pIRβ and pAkt in SMIRKO mouse gingiva were suppressed by 62.5% ($P < 0.05$) and 56.1% ($P < 0.001$), respectively (Fig. 1*C–E*), whereas insulin-induced pErk levels were not impaired (Fig. 1*F*). IGF-1–induced pIGF1Rβ and pAkt levels were decreased only at IGF-1 = 100 nmol/L (both at $P < 0.05$) in the gingiva from SMIRKO mice compared with WT mice (Fig. 1*G–J*).

Comparative Analysis of Periodontitis Pathology

The severity of silk ligature–induced periodontitis showed that the buccal and palatal net bone loss was lower on day 4 but significantly increased by 64.1 and 100% on day 14 in SMIRKO mice compared with WT mice (Fig. 2*A* and *B*) ($P < 0.01$ to ~0.001). The number of TRAP (+) osteoclasts was increased by 60% in ligatured SMIRKO mice compared with WT mice on day 14 (Fig. 2*C* and *D*) ($P < 0.05$), but no differences were found without ligature. Overexpression of Cre recombinase did not affect the alveolar bone loss (Supplementary Fig. 4). The capacity of differentiation into osteoclasts in BMDMs was similar in the two types of mice (Fig. 2*E* and *F*).

Bacterial Clearance and Inflammatory Responses After Ligature

Bacterial load measured by eubacterial 16*S* gene expression in the SMIRKO mouse gingiva was higher than in WT mice on day 4 (Fig. 2*G*) ($P < 0.05$). Both neutrophils ($CD45^+CD3^-CD19^-CD11b^+Gr\text{-}1^+SCC^{low}$) and monocytes ($CD45^+CD3^-CD19^-CD11b^{midhigh}Gr\text{-}1^{mid}$) on day 4 after ligature were lower ($P < 0.05$), but they were higher on day 14 in the gingiva of SMIRKO mice (Fig. 2*H*) ($P = 0.051$), whereas T and B lymphocyte counts were not significantly altered (Supplementary Fig. 5*A*). Splenic, blood, and bone marrow neutrophils, but not other inflammatory cells, were increased in response to ligature, but were not different from baseline in WT and SMIRKO mice (Supplementary Fig. 5*B–D*).

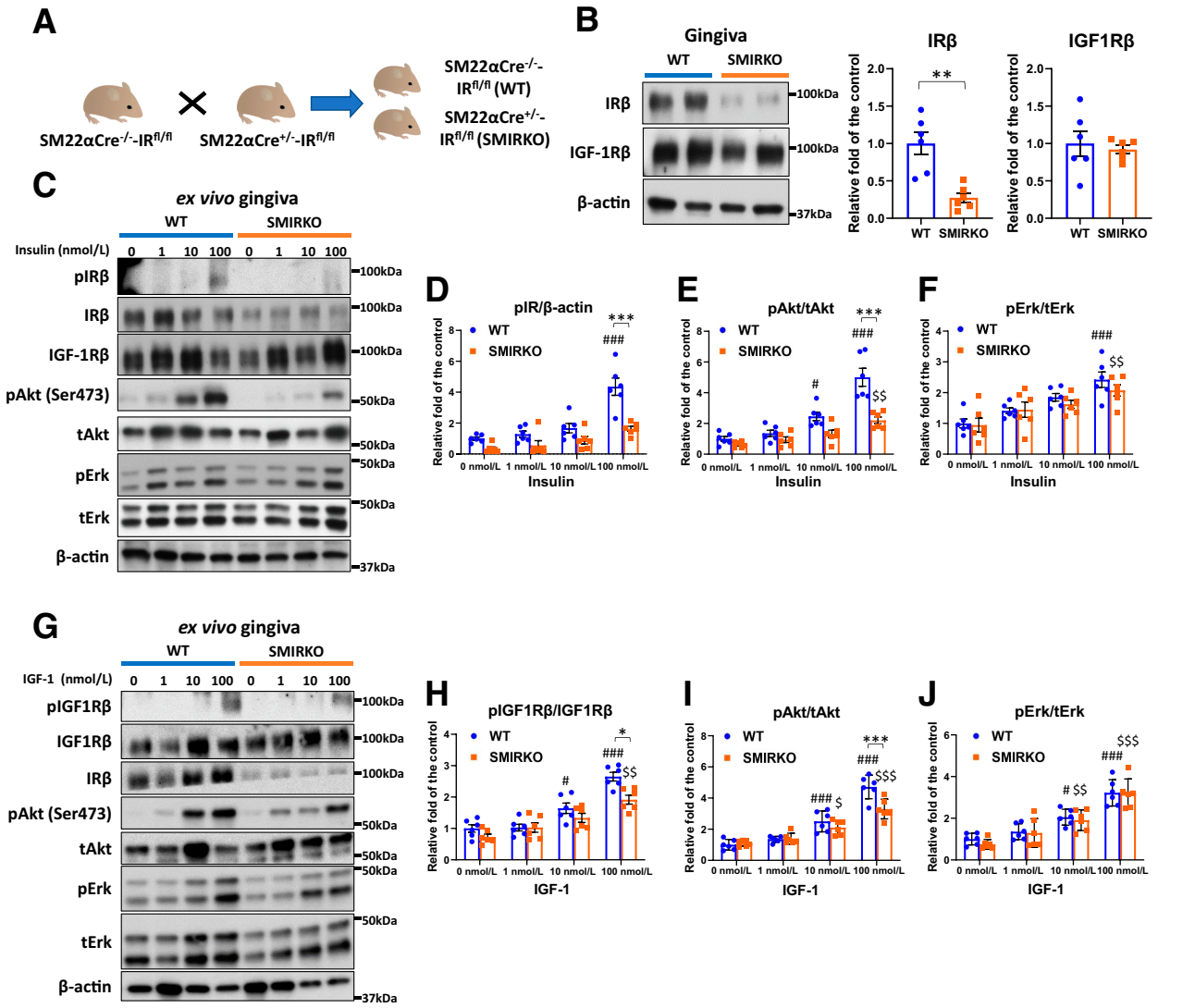

Figure 1—IR expression and insulin/IGF-1 signaling in the gingiva of WT and SMIRKO mice. *A*: A schema of breeding between WT and SMIRKO mice. *B*: IRβ and IGF-1Rβ expression levels in the gingiva of WT and SMIRKO mice ($N = 6$). *C–F*: Insulin-induced signal transduction in the gingiva of WT and SMIRKO mice ($N = 6$). *G–J*: IGF-1–stimulated signal transduction in the gingiva of WT and SMIRKO mice ($N = 6$). $^*P < 0.05$, $^{**}P < 0.01$, $^{***}P < 0.001$. #$P < 0.05$, ###$P < 0.001$ versus WT 0 nmol/L. $$P < 0.05$, $$$P < 0.01$, $$$$P < 0.001$ versus SMIRKO 0 nmol/L. Blue circle, WT; orange square, SMIRKO.

Multiple inflammatory (CXCL1, CXCL2, MCP-1, TNFα, IL-1β, and IL-17A) and osteoclastogenesis-related (RANKL and OPG) genes were upregulated by ligature with peaks on days 4 and 7 in WT mice (Fig. 2*I*). However, in the SMIRKO mice, the gingival expression of all these inflammatory cytokines was lower on day 4 but higher on day 14 after ligature. This delayed expression was confirmed in the protein changes of CXCL1, which were lowered on day 4 ($P < 0.01$) and elevated on day 14, comparing SMIRKO to WT mice (Fig. 2*J*).

Characterizing Periodontitis and Cytokines in HFD-Fed Mice

To support the idea that male SMIRKO mice are mimicking the changes of insulin resistance induced by obesity and diabetes, we studied the effect of HFD in mice (15). Male HFD-fed mice exhibited significant weight gain, insulin resistance measured by IPITT, and mild diabetes measured by IPGTT (Supplementary Fig. 6*A–E*). Fasting insulin levels, but not IGF-1 levels, were elevated in HFD-fed mice compared with RD-fed mice (Supplementary Fig. 6*F* and *G*). No systemic differences were noted between mice with and without ligature (Supplementary Fig. 6*A–C*, *F*, and *G*). IRβ levels were downregulated mice by 63% in the gingiva of HFD-fed mice ($P < 0.05$), but the expression of VCAM1 ($P < 0.05$) and ICAM1 levels was increased compared with RD-fed mice (Fig. 3*A–D*). Insulin-induced pAkt and pErk were reduced significantly by 37 and 37%, respectively, in the gingiva of HFD-fed mice compared with RD mice (Fig. 3*E–G*).

Ligature-induced bone loss in HFD-fed mice was lower on day 4 but was greater by 45% on day 14 compared with

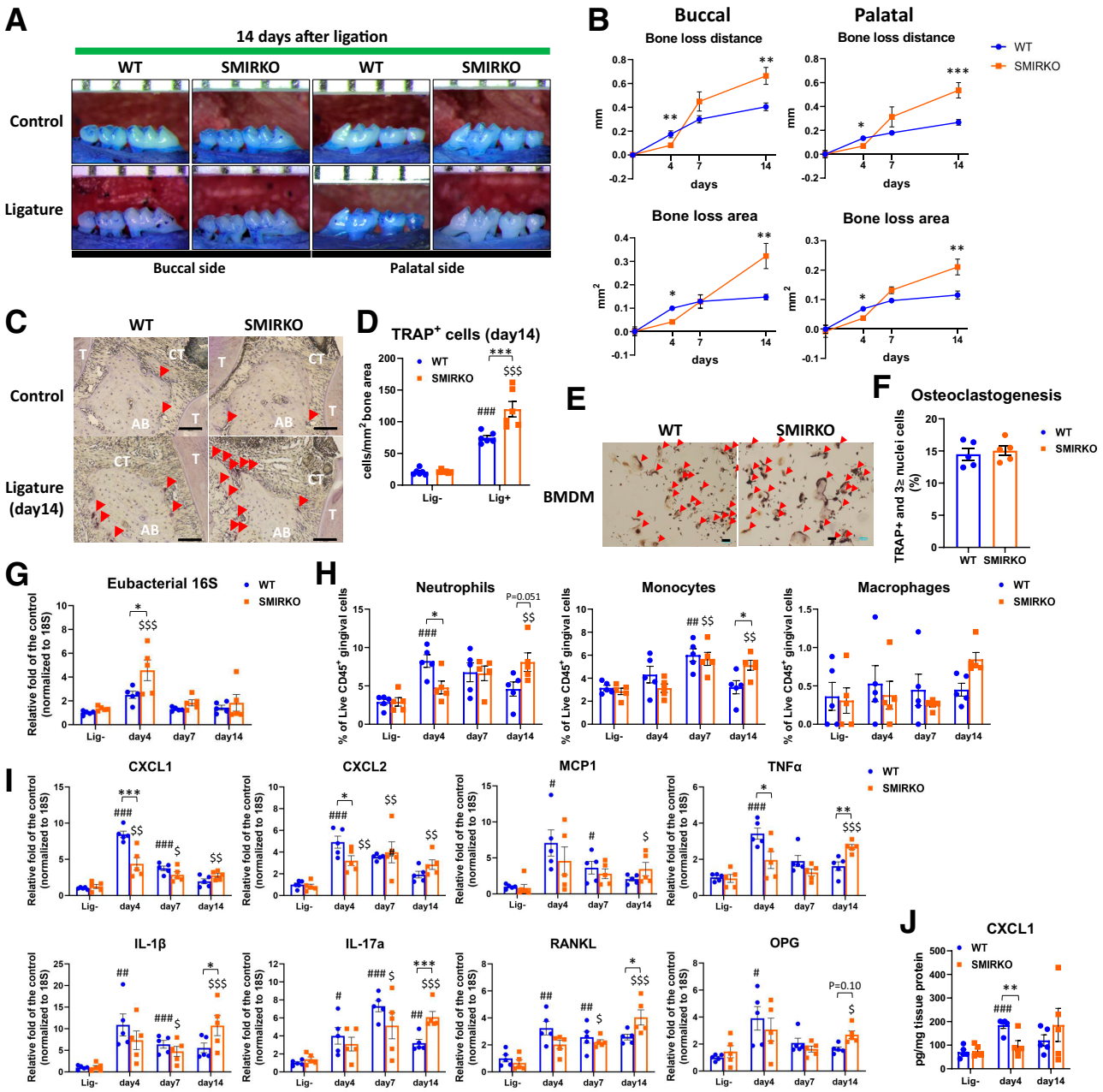

Figure 2—Exacerbation of ligature-induced experimental periodontitis in SMIRKO mice via delay in neutrophil recruitment. *A*: Representative images of maxillae from WT and SMIRKO mice with or without ligature at day 14 after ligation. *B*: Net bone loss distance and area in WT and SMIRKO mice after ligation ($N = 6$). *C* and *D*: Representative images and quantification of TRAP stain in WT and SMIRKO mice at 14 days after ligation ($N = 6$). Scale bar = 100 μm. Red arrows show TRAP-positive cells. *E* and *F*: Representative microphotographs and quantification of TRAP stain in differentiated BMDMs into osteoclasts in WT and SMIRKO mice ($N = 5$). Red arrows show osteoclasts. *G*: Eubacterial 16S expressions ($N = 5$); *H*: immune cell populations (N = 5); *I*: qPCR data ($N = 5$); and *J*: CXCL1 protein levels ($N = 5$) in the gingiva of WT and SMIRKO mice after ligation. *$P < 0.05$, **$P < 0.01$, ***$P < 0.001$. #$P < 0.05$, ##$P < 0.01$, ###$P < 0.001$ versus WT lig-, \$$P < 0.05$, \$\$$P < 0.01$, \$\$\$$P < 0.001$ versus SMIRKO lig-. Blue circle, WT; orange square, SMIRKO; lig-, without ligature.

RD-fed mice ($P < 0.05$ and $P < 0.001$, respectively) (Fig. 3*H* and *I*). The number of osteoclasts was elevated by 24% in HFD-fed mice compared with RD-fed mice ($P < 0.01$) (Fig. 3*J* and *K*).

In the gingiva of HFD-fed mice, eubacterial 16S levels were higher at all time points compared with RD-fed mice (Fig. 3*L*). Neutrophil recruitment was significantly lower by 45% in the gingiva of HFD-fed mice at day 4 but was greater at day 14 compared with RD-fed mice (Fig. 3*M*). Gingival monocyte and macrophage numbers were significantly higher in HFD-fed mice at all time points, compared with RD-fed mice, which peaked at day 7 (Fig. 3*M*), while T and B lymphocyte counts were not changed (Supplementary Fig. 7*A*). Systemically, neutrophils in the spleen, blood, and bone marrow were not different between RD-fed and HFD-fed mice (Supplementary Fig. 7*B–D*), although some elevations

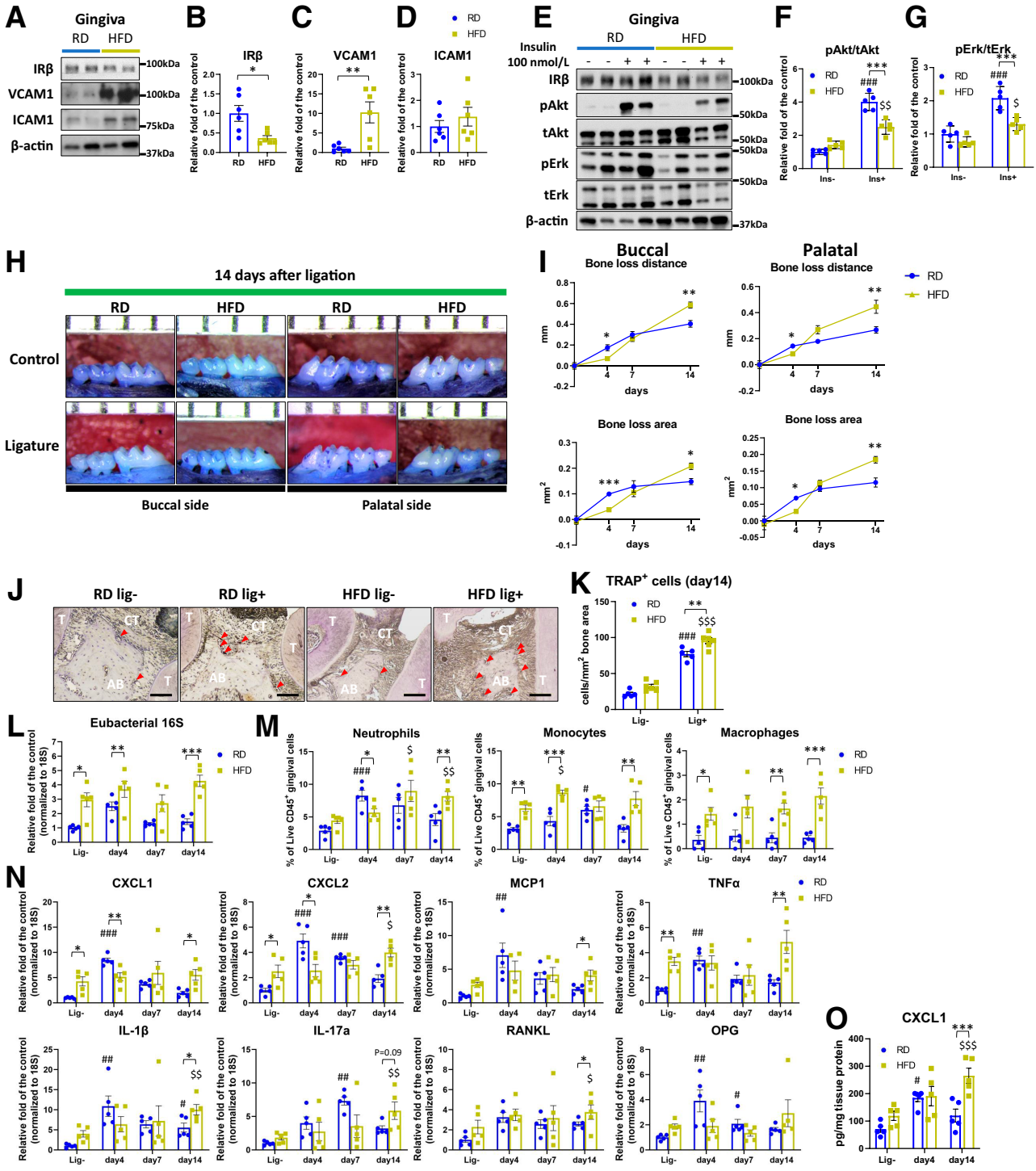

Figure 3—Gingival insulin resistance and exacerbation of ligature-induced experimental periodontitis in HFD-fed mice via dysregulation in neutrophil recruitment. *A–D*: IRβ, VCAM1, and ICAM1 expression levels in the gingiva of RD and HFD-fed mice ($N = 6$). *E–G*: Ex vivo insulin stimulated signal transduction in the gingiva of RD and HFD-fed mice ($N = 5$). *H* and *I*: Representative images of maxillae net bone loss distance and area from RD and HFD-fed mice with or without ligature at day 14 after ligation ($N = 6$). *J* and *K*: Representative images and quantification of TRAP stain in RD and HFD-fed mice at 14 days after ligation ($N = 6$). Scale bar = 100 μm. *L*: Eubacterial 16S expressions ($N = 5$); *M*: immune cell populations ($N = 5$); *N*: qPCR data ($N = 5$); and *O*: CXCL1 protein levels ($N = 5$) in the gingiva of RD and HFD-fed mice after ligation. $*P < 0.05$, $**P < 0.01$, $***P < 0.001$. $\#P < 0.05$, $\#\#P < 0.01$, $\#\#\#P < 0.001$ versus RD-fed lig-, $\$P < 0.05$, $\$\$P < 0.01$, $\$\$\$P < 0.001$ versus HFD-fed lig-. Blue circle, RD-fed; yellow square, HFD-fed; lig-, without ligature.

of monocyte/macrophage levels were observed on days 4 and 7 in the HFD-fed mice (Supplementary Fig. 7*B–D*).

At baseline, gene expression of CXCL1, CXCL2, TNFα, IL-1β, IL-17a, and RANKL in the gingiva of male HFD-fed mice was higher, compared with male RD-fed mice. The expression of inflammatory cytokines peaked at day 4 after ligature in RD-fed mice, but they remained elevated and did not peak until day 14 in HFD-fed mice (Fig. 3*N*). The protein levels of CXCL1 were higher in HFD-fed mice than RD-fed mice at day 14 (Fig. 3*O*) ($P < 0.001$).

Gingiva CXCL1 Overexpression on Bone Loss and Periodontitis

CXCL1 mRNA expression in murine GFs was specifically increased by sixfold using intragingival injection of adenovirus containing murine CXCL1 (AdCXCL1) compared with uninfected GFs or those infected with adeno-CMV-null viral vectors (AdCMV) (Supplementary Fig. 8*A*). There was increased expression of neutrophil-selective enzyme myeloperoxidase and CD11b, a monocyte marker, which remained elevated 7 days after AdCXCL1 infection compared with AdCMV infection (Supplementary Fig. 8*B*).

Bacterial clearance, measured by eubacterial 16S rRNA (Fig. 4*A*), was significantly lower in the gingiva of SMIRKO and HFD-fed mice compared with WT and RD-fed mice, respectively, at days 4 and 14. However, after elevating CXCL1 expression by AdCXCL1 infection, eubacterial 16S levels in the SMIRKO and HFD-fed mice were significantly lower than in mice infected with AdCMV and comparable to those of respective controls of male WT and RD-fed mice (Fig. 4*A*).

Delays of neutrophil recruitment into the gingiva, exhibited by male SMIRKO and HFD-fed mice, compared with male WT and RD-fed mice, respectively, on days 4 and 14 were normalized by intragingival infection of AdCXCL1 compared with AdCMV (Fig. 4*B*). Similarly, the number of monocytes, macrophages, and B cells was normalized to WT mice with AdCXCL1 overexpression on day 14 (Supplementary Fig. 9).

Expression of CXCL1, TNFα, and IL-1β in the gingiva of SMIRKO and HFD-fed mice infected with AdCXCL1 was normalized on day 4 and significantly lower on day 14 compared with mice with AdCMV (Fig. 4*C–E* and Supplementary Fig. 10). Similarly, ligature-induced bone losses in SMIRKO and HFD-fed mice injected with AdCXCL1 measured at day 14 were comparable with each other and lower than in WT and RD-fed mice injected with AdCMV ($P < 0.001$) (Fig. 4*F–H* and Supplementary Fig. 11).

Insulin Signaling and Effects in Gingival Myofibroblasts

Primary GFs from male SMIRKO mice showed reductions of IRβ by 91%, but no changes in IGF1Rβ, compared with male WT mice (Fig. 5*A*). No differences were noted in the expression of vimentin, αSMA, and SM22α between GFs from WT and SMIRKO mice, indicating similar levels of differentiation (Fig. 5*B* and Supplementary Fig. 12). Insulin-induced (1–100 nmol/L) pAkt reduced by 38% ($P < 0.001$), but pErk did not, comparing SMIRKO with WT myofibroblasts (Fig. 5*C–E*). IGF-1–induced pIGF1Rβ, pAkt, and pErk were significantly inhibited in GFs from SMIRKO mice, by 29, 35, and 28%, respectively, compared with WT cells (Fig. 5*F–I*).

Cultured GFs from male HFD-fed mice exhibited similar and persistent reductions of IRβ and IGF1Rβ expression, by 50 and 39%, respectively, (Fig. 5*J–L*). Insulin-induced pAkt and pErk were significantly inhibited, by 32 and 27%, respectively, in GFs from HFD-fed mice compared with RD-fed mice (Fig. 5*M* and *N*).

CXCL1 Expression in GFs Induced by LPS and Insulin

Insulin's effect to modulate CXCL1 expression by LPS, a major inducer of CXCL1 expression in bacterial infection, was studied (28). CXCL1 gene expression and protein secretion were strongly induced by a Toll-like receptor 4 (TLR4) ligand, *E. coli* LPS (10 ng/mL), a TLR2 ligand, Pam3CKS4 (100 ng/mL), and a TLR5 ligand, flagellin (10 ng/mL), in mouse GFs (Fig. 6*A* and *B* and Supplementary Fig. 13). LPS-induced CXCL1 gene expression increased by 200-fold at 6 h, with reductions after 12 and 24 h (Fig. 6*A* and *B*. Insulin alone did not affect CXCL1 expression. LPS-induced CXCL1 gene expression at 6 h and protein secretion were significantly lower in GFs from male SMIRKO mice, by 64 and 80%, respectively (Fig. 6*A* and *B*). GFs from HFD-fed mice also showed significant reductions of LPS-induced CXCL1 gene at 6 h and protein expression, by 60 and 50% (Fig. 6*C* and *D*), respectively, when compared with RD-fed cells. Pretreatment of GFs with insulin (100 nmol/L) enhanced LPS, Pam3CKS4, and flagellin-induced CXCL1 expression in WT-GFs by 1.5-fold at 6 h, but not in GFs from both SMIRKO and HFD-fed mice (Fig. 6*A–D* and Supplementary Fig. 13).

The expression of CXCL1 induced by LPS is by binding to TLR with activation of the NF-κB pathway (28). This was confirmed, since LPS, Pam3CSK4, and TNFα-stimulated CXCL1 mRNA and protein expression was inhibited by IKK-β inhibitor BAY 11-7082, but not by JNK inhibitor SP600125 (Fig. 6*E*). Inhibitors of PI3K, wortmannin (Supplementary Fig. 14*A*), did not affect LPS-induced CXCL1 expression, but completely inhibited insulin-mediated enhancement of LPS's effect (Fig. 6*F* and *G*). MAP kinase inhibitor PD98059 tended to decrease insulin's additive effects on CXCL1 expression. Actions of insulin via the Akt pathway were studied further by shAkt transfection, which reduced Akt by 72%, compared with shCMV (Supplementary Fig. 14*B*), and inhibited completely insulin-enhanced LPS-stimulated CXCL1 expression (Fig. 6*H* and *I*).

In human GFs, LPS significantly increased CXCL1 expression at 6 h and decreased it at 12 and 24 h. Insulin alone was ineffective, but it significantly elevated LPS-induced CXCL1 mRNA and protein expression, by 47% ($P < 0.001$) and 41% ($P < 0.01$), respectively (Fig. 6*J* and *K*).

GFs exposed to insulin (100 nmol/L) for 48 or 120 h induced loss of insulin activation of p-Akt (Supplementary Fig. 15*A–E*) and attenuated insulin-enhanced LPS-induced CXCL1 gene and protein expression significantly (Supplementary Fig. 15*F–H*).

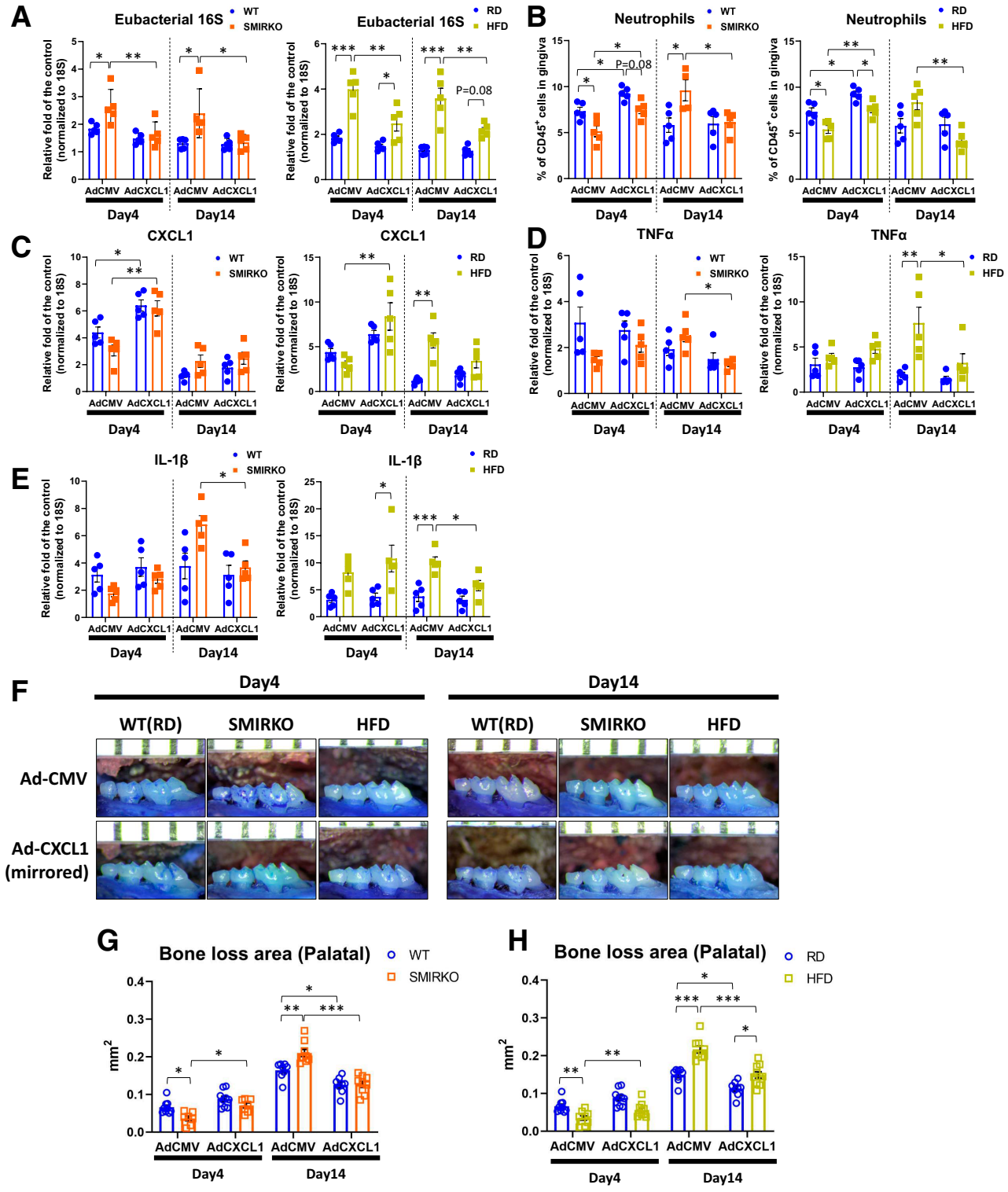

Figure 4—Normalization of ligature-induced experimental periodontitis in SMIRKO and HFD-fed mice by overexpression of intragingival adenoviral CXCL1. *A*: Eubacterial 16S expressions ($N = 5$); *B*: neutrophil populations ($N = 5$); *C*: CXCL1 ($N = 5$); *D*: TNFα ($N = 5$); and *E*: IL-1β mRNA expressions in the gingiva from WT, SMIRKO, and HFD-fed mice after ligations with intragingival adenoviral CMV or CXCL1 overexpression ($N = 5$). *F*: Representative photographs and *G* and *H*: net bone loss area of each mouse with intragingival adenoviral CMV or CXCL1 overexpression ($N = 7$–10). *$P < 0.05$, **$P < 0.01$, ***$P < 0.001$. Blue circle, WT (RD-fed); orange square, SMIRKO; yellow square, HFD-fed.

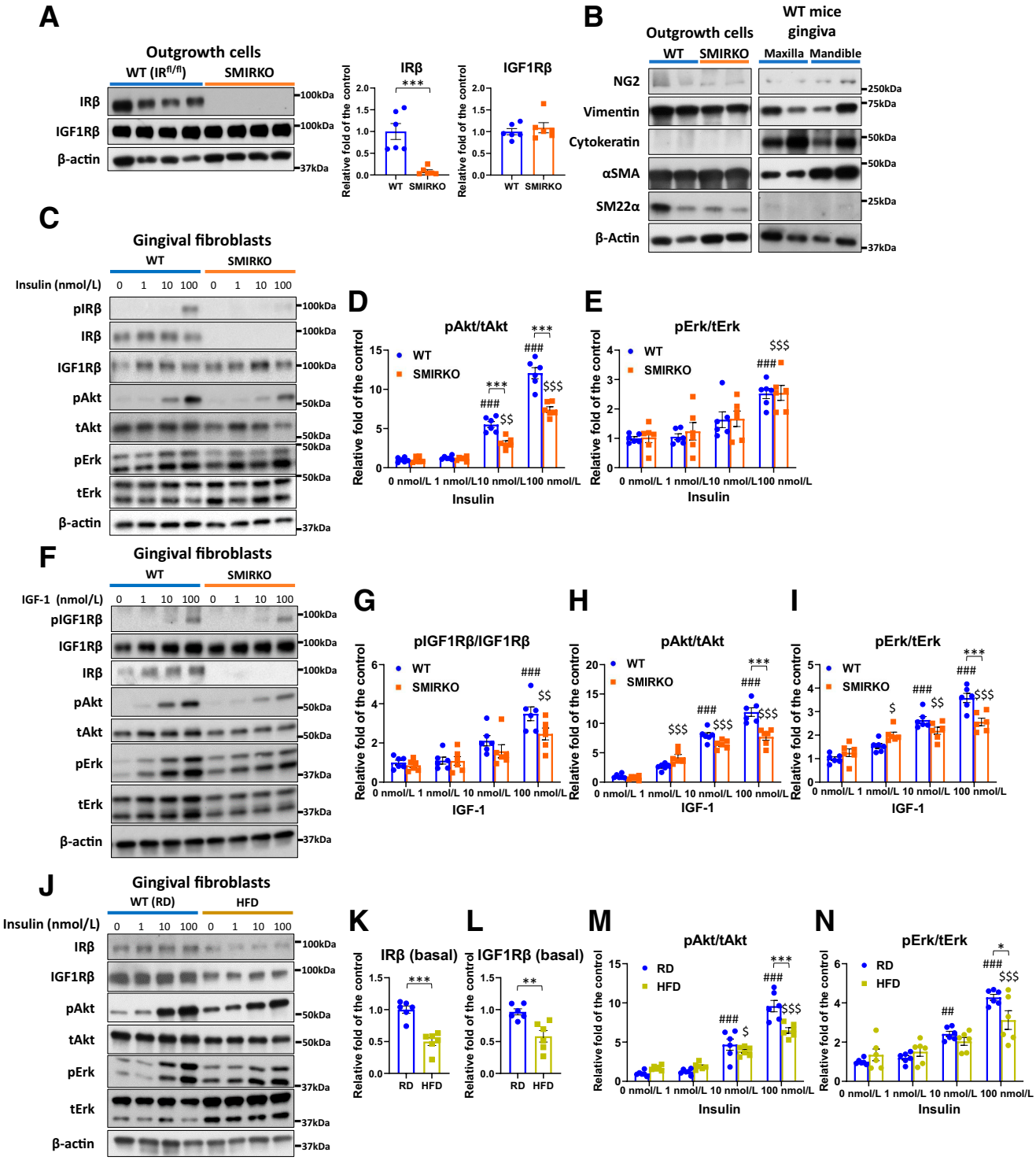

Figure 5— Insulin and IGF-1 signaling in GFs from WT (RD-fed), SMIRKO, and HFD-fed mice. *A*: IRβ and IGF-1Rβ expressions in gingival outgrowth cells from WT and SMIRKO mice ($N = 6$). *B*: Confirmation of cell markers in GFs. *C–E*: Insulin signal transduction and *F-I*: IGF-1 signal transduction in GFs from WT and SMIRKO mice ($N = 6$). *J–L*: Basal IRβ and *N*: basal IGF1Rβ expression ($N = 6$), and *M* and *N*: insulin signal transduction in GFs from RD and HFD-fed mice ($N = 6$). $^{*}P < 0.05$, $^{**}P < 0.01$, $^{***}P < 0.001$. ##$P < 0.01$, ###$P < 0.001$ versus WT (RD-fed) 0 nmol/L, \$$P < 0.05$, \$\$$P < 0.01$, \$\$\$$P < 0.001$ versus SMIRKO or HFD-fed 0 nmol/L. Blue circle, WT (RD-fed); orange square, SMIRKO; yellow square, HFD-fed.

NF-κB Activation on CXCL1 Expression in GFs

Protein expression of TLR2 and TLR4 was not statistically different in GFs from all three types of male mice at baseline and after LPS stimulation, except TLR2 levels were decreased at 1,000 ng/mL (LPS) in GFs from male HFD-fed mice (Fig. 7*A* and *B*). Activation of NF-κB pathway in WT mice showed that LPS increased pTAK1, IκBα degradation, and p-p65 significantly, from 10 to 1,000 ng/mL (Fig. 7*A* and *B*). Basal

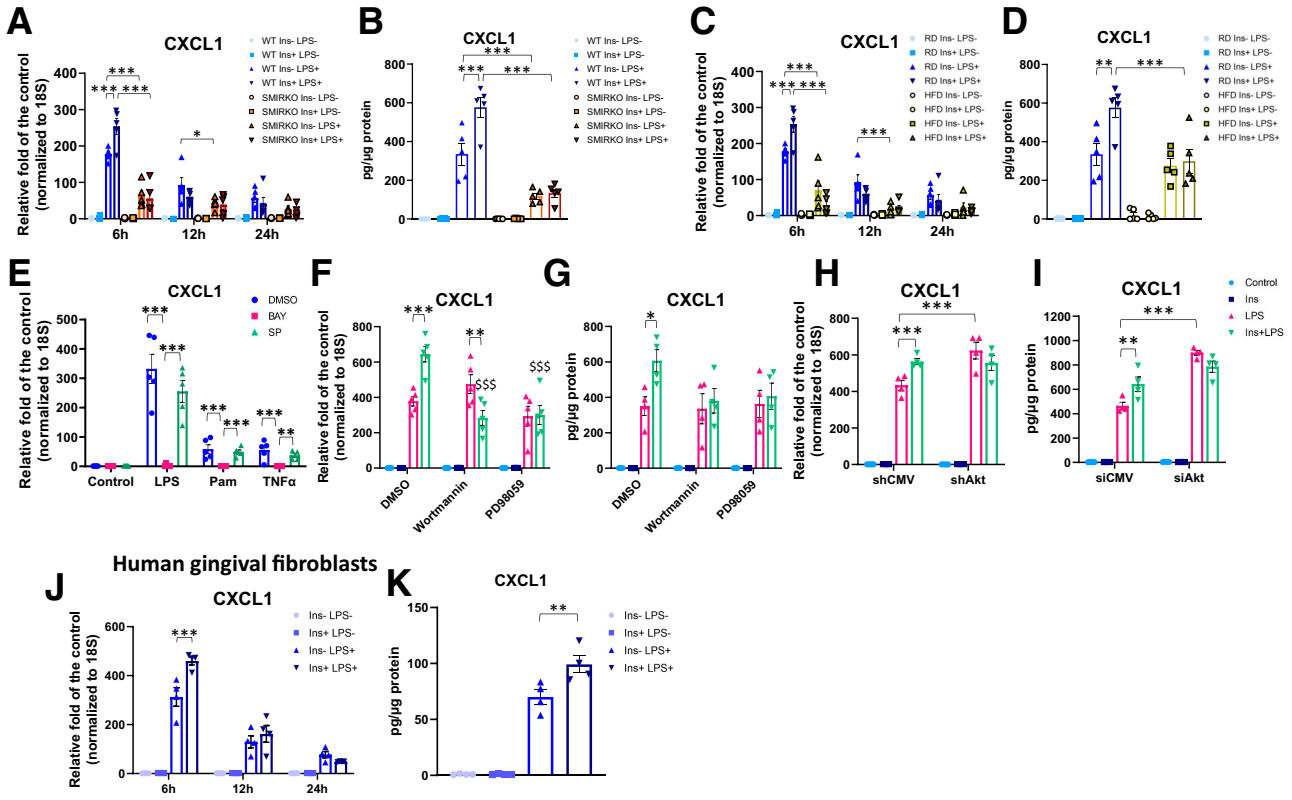

Figure 6—Insulin transiently enhanced LPS-induced CXCL1 expression in GFs but not in SMIRKO and HFD-fed mice. *A*: qPCR ($N = 5$) and *B*: ELISA of CXCL1 expression in and production from GFs of WT and SMIRKO mice ($N = 5$). *C*: qPCR and *D*: ELISA of CXCL1 expression and production from GFs of RD and HFD-fed mice ($N = 5$). *E*: Confirmation of LPS, Pam3CSK4 (Pam), and TNFα (10 ng/mL each) induced pathway to express CXCL1 in GFs ($N = 5$). *F*: qPCR ($N = 5$) and *G*: ELISA in CXCL1 levels in and from GFs treated with wortmannin or PD98059 ($N = 4$). *H*: qPCR ($N = 4$) and *I*: ELISA in CXCL1 expression in GFs treated with shAkt1 or control vector (shCMV) ($N = 4$). *J*: Effect of insulin on LPS-induced CXCL1 expression ($N = 4$) and *K*: productions from human primary GFs ($N = 4$). *$P < 0.05$, **$P < 0.01$, ***$P < 0.001$. $$$$P < 0.001$ versus Ins+LPS-treated GFs.

levels of p-TAK in GFs from SMIRKO and HFD-fed mice ($P < 0.05$) were higher (by twofold to threefold) than those from WT mice. LPS stimulation of p-TAK was comparable to cells from SMIRKO and HFD-fed mice compared with WT mice. Basal levels of IκBα between WT and SMIRKO GFs were not different, but they were elevated in cells from HFD-fed mice ($P < 0.05$). LPS (10 to 1,000 ng/mL) reduced IκBα protein levels significantly, by up to 75%, in WT mice, but by 74 and only 20% in GFs from SMIRKO and HFD-fed mice, respectively (Fig. 7*A* and *B*). In contrast, basal p-p65/p65 levels were significantly reduced in GFs from SMIRKO and HFD-fed mice compared with WT mice (Fig. 7*A* and *B*). LPS stimulated p-p65 levels by 1.6- to 2.6-fold in GFs from WT cells, but was blunted significantly in GFs from both SMIRKO and HFD-fed mice, with the greatest reductions from the latter (Fig. 7*B*). However, LPS stimulation of pJNK did not differ among the GFs from WT, SMIRKO, and HFD mice (Fig. 7*A* and *B*). Insulin-enhanced LPS actions increased pTAK1/tTAK1, reduced IκBα protein, and significantly increased p-p65 levels ($P < 0.05$) in WT mice, but not in GFs from SMIRKO and HFD mice (Fig. 7*C* and *D*).

DISCUSSION

These results have established, for the first time, that IR in GF can enhance CXCL1 expression via the NF-κB pathway and mitigate the severity of periodontitis and even bone loss.

The physiological importance of insulin enhancement of LPS induction of CXCL1 expression is supported by the findings that HFD manifested similar reductions of IR and its signaling via the pAkt pathway in the gingiva, and exhibited exacerbation of periodontitis and bone loss compared with WT mice. Thus, we surmised that the reductions in pAkt by the loss of IR as found in both male SMIRKO and HFD-fed mice mediated the delay in bacterial clearance and excessive bone loss in mouse models of periodontitis.

Excessive bone loss in SMIRKO mice was related to the delay in bacterial clearance that resulted from the diminished chemotaxis of neutrophils and monocytes into the gingiva, which remained chronically elevated. This delay and the persistent infection were similar to inflammatory cytokine expression with the elevation of TNFα, IL-1β, and IL-17A, which are known potent inducers of osteoclast formation as substantiated by the changes in RANKL and OPG (29–32). The mechanism for delayed resolution of the bacterial infection in the gingiva of SMIRKO mice was related to the decreased expression of CXCL1, CXCL2, and MCP-1 and the delay in the recruitment of neutrophils and monocytes. Previous studies have shown that recruitment of neutrophils and their actions are critical for resolving periodontitis and wound healing (1,33–36). However, this

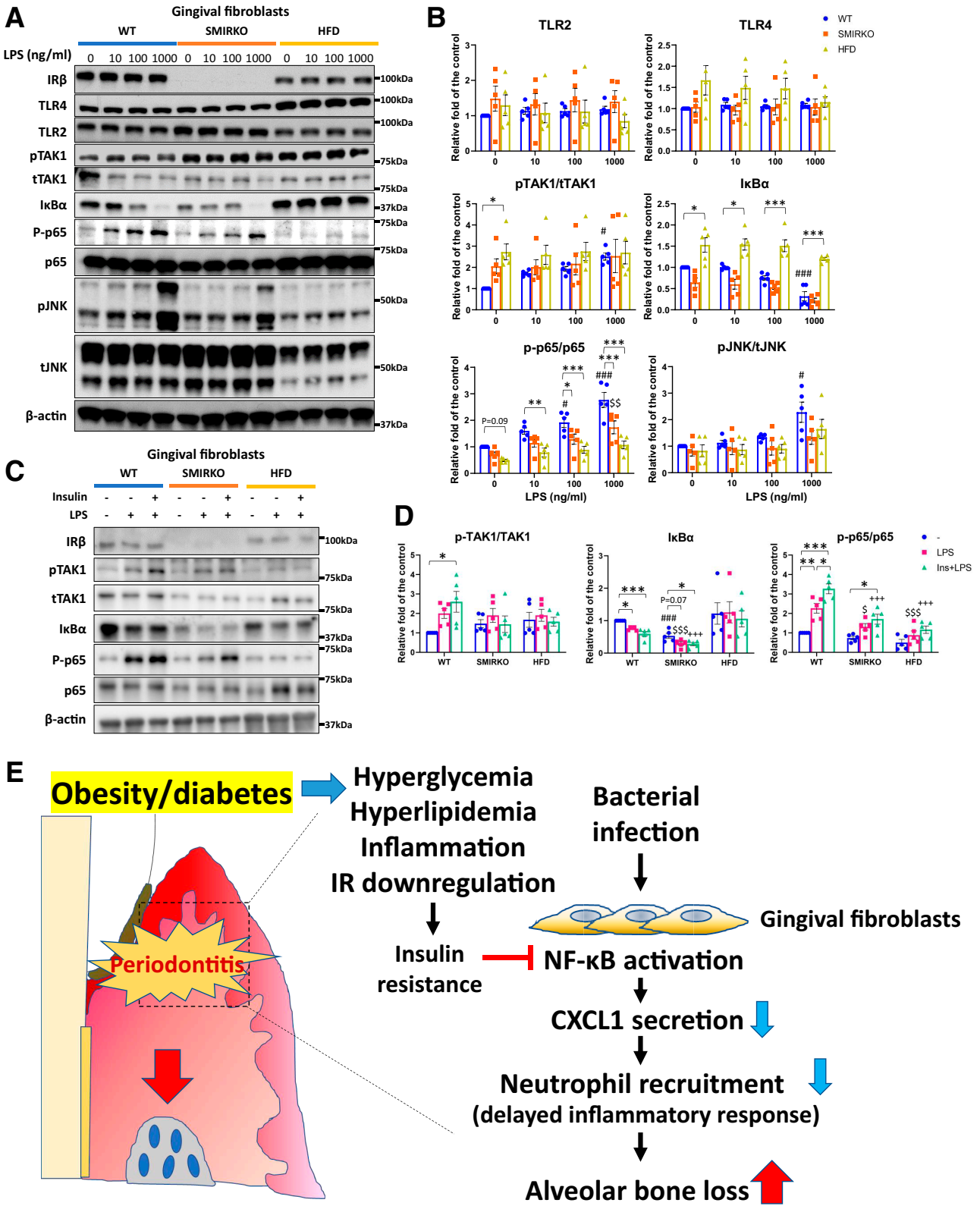

Figure 7— Endotoxin tolerance and insulin-enhanced LPS-mediated NF-κB activation in GFs from SMIRKO and HFD mice. *A*: Representative images and *B*: quantification data of LPS-induced signal transduction in GFs from WT (RD-fed), SMIRKO, and HFD-fed mice in dose-dependent manner ($N = 5$). *C*: Representative images and *D*: quantification blots of 100 ng/mL LPS-induced NF-κB pathway activation in the presence or absence of insulin (100 nmol/L) pretreatment ($N = 5$). *E*: A schema of conclusion of the study. $^{*}P < 0.05$; $^{**}P < 0.01$; $^{***}P < 0.001$. $\#P < 0.05$, $\#\#\#P < 0.001$ versus WT (RD-fed) controls. $\$P < 0.05$, $\$\$P < 0.01$, $\$\$\$P < 0.001$ versus control of GFs from SMIRKO mice in *B* and LPS-treated GFs of WT mice in *D*. $+++P < 0.001$ versus Ins+LPS-treated GFs from WT mice in *D*. In *B*: blue circle, WT (RD-fed); orange square, SMIRKO; yellow square, HFD-fed. In *D*: blue circle, untreated; magenta square, LPS-treated; green triangle, Ins+LPS-treated in GFs from WT (RD-fed) mice.

is the first report of IR regulating CXCL1 expression in any tissues and its relationship to delayed neutrophil recruitment in wound healing and periodontitis. We suggest that loss of IR signaling in insulin resistance and diabetes decreased CXCL1 expression and is responsible for the delayed neutrophil recruitment and bacterial clearance with persistent inflammation in gingiva of HFD-fed and diabetic mice, resulting in excessive bone loss. Since only CXCL1 and CXCL2 expression was decreased in HFD-fed mice, and not MCP-1 (Fig. 3*N*), the delayed recruitment of neutrophils is likely the major defect for the chronic inflammation and bone loss in both male SMIRKO and HFD-fed mice. However, in HFD-fed mice, baseline levels of bacteria, macrophages, monocytes, and various inflammatory cytokines were already elevated before periodontal injury, and bone loss was not present (Fig. 3*L–O*), which suggest that insulin resistance caused by HFD can induce chronic elevation of bacterial load and increased inflammatory cytokine levels in gingiva and systemically.

The idea that CXCL1 reduction is responsible for the excessive alveolar bone loss in male SMIRKO and HFD-fed mouse models of periodontitis is strongly supported by the selective overexpression of CXCL1 in the gingiva with adenoviral CXCL1, which corrected the abnormalities of bacteria clearance, elevations of inflammatory cytokines in both models, and prevented chronic inflammatory changes responsible for bone loss.

Mechanistic studies in GFs confirmed that insulin's effect requires LPS and is due to its activation of the NF-κB pathway through TLR2/TLR4/TLR5, which is the major pathway for LPS to activate CXCL1 expression (Supplementary Fig. 13) (26). This insulin action is likely mediated through its activation of the pAkt pathway rather than MAPK activation, since inhibitors of pAkt selectively inhibit insulin's additive effect on LPS induction of CXCL1 without inhibiting LPS activation (Fig. 6*F* and *G*). However, inhibition of MAP kinase reduced LPS-induced CXCL1 expression completely. Thus, loss of insulin actions to enhance LPS's induction of CXCL1 expression in HFD-fed diabetic mice is related to selective inhibition of insulin signaling of the Akt pathway, as reported in multiple cardiovascular and other insulin responsive tissues (37).

The study using GFs from both male SMIRKO and HFD-fed mice provided interesting findings that not only are insulin's additive actions reduced, but LPS induction of CXCL1 alone was also dramatically reduced (Fig. 6*A–D*). These findings suggest that IR and insulin action could be mediating its actions at multiple points of LPS activation of the NF-κB pathway. One of insulin's actions is through pAkt activation, as described. However, the substantial loss of LPS induction of CXCL1 in GFs from SMIRKO mice suggests that loss of IR can also reduce LPS activation of NF-κB as measured by IκBα and p-p65/p65. Further, the persistence of these signaling abnormalities of IR and LPS in cultured GF of SMIRKO and HFD-fed mice indicated the retention of metabolic memory, possibly at the epigenetic levels, as reported in other tissues (38–40). Chronic exposure to insulin clearly attenuated insulin's enhancing effect of LPS-induced CXCL1 expression in mouse GFs, which is likely due to downregulation of IR and its actions reported in many types of cells (Supplementary Fig. 15) (41). Thus, it is possible that hyperinsulinemia due to HFD partially contributed to reduction of CXCL1 expression.

Our study has several limitations. First, only male mice were used for the experiments, since male gender is an independent risk factor for periodontitis and short reproductive cycle and hormone changes may affect the progression of periodontitis during the 14-day study. Future study will be needed to determine whether the finding of reductions of CXCL1 expression associated with insulin resistance and mild diabetes is also applicable in female mice. Second, our study focused on obesity, insulin resistance, and type 2 diabetes, but not on insulin deficiency diabetes. Since hyperglycemia likely also has inhibitory effects on insulin's activation of the pAkt pathway (42–44), future studies will be needed to address whether hyperglycemia and hypoinsulinemia can also cause reductions of CXCL1 expressions in the gingiva.

These data provide the first evidence of insulin's actions to enhance LPS activation in any cell type and suggest enhancing CXCL1 expression as a potential therapeutic direction for periodontitis and impaired wound healing in diabetes.

Acknowledgments. The authors are grateful for the support of Dr. C. Ronald Kahn at Joslin Diabetes Center for IR floxed mice. Additionally, the authors thank Dr. Robert J. Genco at Department of Oral Biology, School of Dental Medicine, State University of New York at Buffalo (Buffalo, NY) for inspiration regarding the association of periodontitis and diabetes. The authors thank the Joslin Diabetes Center's DRC for access to Animal Physiology Core, Molecular Core, and Flow Core.

Funding. T.S. is the recipient of research fellowships (Hiroo Kaneda Scholarship, Sunstar Foundation, Japan, and Mary K. Iacocca Foundation), a Mary K. Iacocca Research Fellowship Award, and the Japanese Society of Periodontology Young Investigator Research Fund. Support was provided to G.L.K. by the NIH/National Institute of Diabetes and Digestive and Kidney Diseases (NIDDK) Diabetes Research Center grant 1DP3-DK-094333-01 and NIH grant R01 DK053105. S.O. is a recipient of a Kaneda Hiroo Fellowship from Sunstar Foundation and is supported by the Uehara Memorial Foundation. J.F. was supported by a Mary K. Iacocca Research Fellowship Award and American Diabetes Association Scientific Sessions Young Investigator Award. Q.L. was supported by the American Diabetes Association Mentor-Based Postdoctoral Fellowship Award. Animal Physiology Core, Molecular Core, and Flow Core were supported by NIH grant 5P30-DK-036836.

Duality of Interest. No potential conflicts of interest relevant to this article were reported.

Author Contributions. T.S. performed most of the experiments and wrote the first draft of the manuscript. S.O., Y.Z., A.I., K.P., Q.L., H.Y., T.Z., K.S., R.S.-L., J.F., and W.I.-H. assisted in some studies and reviewed the manuscript. K.M., H.H., T.E.V.D., and F.N. provided advice on the study using obese model mice and review of the manuscript. G.L.K. conceived the project, designed the experiments, supervised all studies, and wrote the manuscript. G.L.K. is the guarantor of this work and, as such, had full access to all the data in the study and takes responsibility for the integrity of the data and the accuracy of data analysis.

Prior Presentation. Parts of this study were presented in poster form at the American Diabetes Association 2019 Annual Meeting (San Diego, CA), 7–11 June 2019.

References

1. Martin P, Nunan R. Cellular and molecular mechanisms of repair in acute and chronic wound healing. Br J Dermatol 2015;173:370–378
2. Patel S, Srivastava S, Singh MR, Singh D. Mechanistic insight into diabetic wounds: pathogenesis, molecular targets and treatment strategies to pace wound healing. Biomed Pharmacother 2019;112:108615
3. Nakamura M, Ojima T, Nagahata T, et al. NIPPON DATA2010 Research Group. Having few remaining teeth is associated with a low nutrient intake and low serum albumin levels in middle-aged and older Japanese individuals: findings from the NIPPON DATA2010. Environ Health Prev Med 2019;24:1
4. Hirotomi T, Yoshihara A, Ogawa H, Miyazaki H. Number of teeth and 5-year mortality in an elderly population. Community Dent Oral Epidemiol 2015;43:226–231
5. Graves DT, Ding Z, Yang Y. The impact of diabetes on periodontal diseases. Periodontol 2000 2020;82:214–224
6. Sanz M, Ceriello A, Buysschaert M, et al. Scientific evidence on the links between periodontal diseases and diabetes: consensus report and guidelines of the joint workshop on periodontal diseases and diabetes by the International Diabetes Federation and the European Federation of Periodontology. J Clin Periodontol 2018;45:138–149
7. Van Dyke TE, Serhan CN. Resolution of inflammation: a new paradigm for the pathogenesis of periodontal diseases. J Dent Res 2003;82:82–90
8. Brem H, Tomic-Canic M. Cellular and molecular basis of wound healing in diabetes. J Clin Invest 2007;117:1219–1222
9. Khader YS, Dauod AS, El-Qaderi SS, Alkafajei A, Batayha WQ. Periodontal status of diabetics compared with nondiabetics: a meta-analysis. J Diabetes Complications 2006;20:59–68
10. Parsegian K, Randall D, Curtis M, Ioannidou E. Association between periodontitis and chronic kidney disease. Periodontol 2000 2022;89:114–124
11. Shinjo T, Ishikado A, Hasturk H, et al. Characterization of periodontitis in people with type 1 diabetes of 50 years or longer duration. J Periodontol 2019;90:565–575
12. Polak D, Sanui T, Nishimura F, Shapira L. Diabetes as a risk factor for periodontal disease-plausible mechanisms. Periodontol 2000 2020;83:46–58
13. Nishikawa T, Suzuki Y, Sawada N, et al. Therapeutic potential for insulin on type 1 diabetes-associated periodontitis: analysis of experimental periodontitis in streptozotocin-induced diabetic rats. J Diabetes Investig 2020;11:1482–1489
14. Mizutani K, Park K, Mima A, Katagiri S, King GL. Obesity-associated gingival vascular inflammation and insulin resistance. J Dent Res 2014;93:596–601
15. Amar S, Zhou Q, Shaik-Dasthagirisaheb Y, Leeman S. Diet-induced obesity in mice causes changes in immune responses and bone loss manifested by bacterial challenge. Proc Natl Acad Sci USA 2007;104:20466–20471
16. Muluke M, Gold T, Kiefhaber K, et al. Diet-induced obesity and its differential impact on periodontal bone loss. J Dent Res 2016;95:223–229
17. Kominato H, Takeda K, Mizutani K, et al. Metformin accelerates wound healing by Akt phosphorylation of gingival fibroblasts in insulin-resistant prediabetes mice. J Periodontol 2022;93:256–268
18. Lim SG, Han K, Kim HA, et al. Association between insulin resistance and periodontitis in Korean adults. J Clin Periodontol 2014;41:121–130
19. Smith PC. Role of myofibroblasts in normal and pathological periodontal wound healing. Oral Dis 2018;24:26–29
20. Li Q, Fu J, Xia Y, et al. Homozygous receptors for insulin and not IGF-1 accelerate intimal hyperplasia in insulin resistance and diabetes. Nat Commun 2019;10:4427
21. Nakao Y, Fukuda T, Zhang Q, et al. Exosomes from TNF-α-treated human gingiva-derived MSCs enhance M2 macrophage polarization and inhibit periodontal bone loss. Acta Biomater 2021;122:306–324
22. Abe T, Hajishengallis G. Optimization of the ligature-induced periodontitis model in mice. J Immunol Methods 2013;394:49–54
23. Papathanasiou E, Kantarci A, Konstantinidis A, Gao H, Van Dyke TE. SOCS-3 regulates alveolar bone loss in experimental periodontitis. J Dent Res 2016;95:1018–1025
24. Takeshita S, Kaji K, Kudo A. Identification and characterization of the new osteoclast progenitor with macrophage phenotypes being able to differentiate into mature osteoclasts. J Bone Miner Res 2000;15:1477–1488
25. Li CH, Amar S. Morphometric, histomorphometric, and microcomputed tomographic analysis of periodontal inflammatory lesions in a murine model. J Periodontol 2007;78:1120–1128
26. Dutzan N, Abusleme L, Konkel JE, Moutsopoulos NM. Isolation, characterization and functional examination of the gingival immune cell network. J Vis Exp 2016:53736
27. Park KH, Kim DK, Huh YH, et al. NAMPT enzyme activity regulates catabolic gene expression in gingival fibroblasts during periodontitis. Exp Mol Med 2017;49:e368
28. Jönsson D, Amisten S, Bratthall G, Holm A, Nilsson BO. LPS induces GROα chemokine production via NF-κB in oral fibroblasts. Inflamm Res 2009;58:791–796
29. Bertolini DR, Nedwin GE, Bringman TS, Smith DD, Mundy GR. Stimulation of bone resorption and inhibition of bone formation in vitro by human tumour necrosis factors. Nature 1986;319:516–518
30. Kim JH, Jin HM, Kim K, et al. The mechanism of osteoclast differentiation induced by IL-1. J Immunol 2009;183:1862–1870
31. Kotake S, Udagawa N, Takahashi N, et al. IL-17 in synovial fluids from patients with rheumatoid arthritis is a potent stimulator of osteoclastogenesis. J Clin Invest 1999;103:1345–1352
32. Xiao E, Mattos M, Vieira GHA, et al. Diabetes enhances IL-17 expression and alters the oral microbiome to increase its pathogenicity. Cell Host Microbe 2017;22:120–128.e4
33. Hajishengallis G, Moutsopoulos NM, Hajishengallis E, Chavakis T. Immune and regulatory functions of neutrophils in inflammatory bone loss. Semin Immunol 2016;28:146–158
34. de Oliveira S, Rosowski EE, Huttenlocher A. Neutrophil migration in infection and wound repair: going forward in reverse. Nat Rev Immunol 2016;16:378–391
35. Soehnlein O, Steffens S, Hidalgo A, Weber C. Neutrophils as protagonists and targets in chronic inflammation. Nat Rev Immunol 2017;17:248–261
36. Ryder MI. Comparison of neutrophil functions in aggressive and chronic periodontitis. Periodontol 2000 2010;53:124–137
37. King GL, Park K, Li Q. Selective insulin resistance and the development of cardiovascular diseases in diabetes: The 2015 Edwin Bierman Award Lecture. Diabetes 2016;65:1462–1471
38. LeRoith D, Fonseca V, Vinik A. Metabolic memory in diabetes—focus on insulin. Diabetes Metab Res Rev 2005;21:85–90
39. Reddy MA, Natarajan R. Epigenetic mechanisms in diabetic vascular complications. Cardiovasc Res 2011;90:421–429
40. Al-Rikabi AHA, Tobin DJ, Riches-Suman K, Thornton MJ. Dermal fibroblasts cultured from donors with type 2 diabetes mellitus retain an epigenetic memory associated with poor wound healing responses. Sci Rep 2021;11:1474
41. Artunc F, Schleicher E, Weigert C, Fritsche A, Stefan N, Häring HU. The impact of insulin resistance on the kidney and vasculature. Nat Rev Nephrol 2016;12:721–737
42. King GL, Loeken MR. Hyperglycemia-induced oxidative stress in diabetic complications. Histochem Cell Biol 2004;122:333–338
43. Tomás E, Lin YS, Dagher Z, et al. Hyperglycemia and insulin resistance: possible mechanisms. Ann N Y Acad Sci 2002;967:43–51
44. Brown MS, Goldstein JL. Selective versus total insulin resistance: a pathogenic paradox. Cell Metab 2008;7:95–96